



Published in final edited form as:

*Circ Arrhythm Electrophysiol.* 2020 February ; 13(2): e007586. doi:10.1161/CIRCEP.119.007586.

## Association of Left Atrial High-Resolution Late Gadolinium Enhancement on Cardiac Magnetic Resonance with Electrogram Abnormalities Beyond Voltage in Patients with Atrial Fibrillation

Ling Kuo, MD<sup>1,2</sup>, Erica Zado, PA-C<sup>2</sup>, David Frankel, MD<sup>2</sup>, Pasquale Santangelli, MD, PhD<sup>2</sup>, Jeffrey Arkles, MD<sup>2</sup>, Yuchi Han, MD, MMSc<sup>3</sup>, Francis E. Marchlinski, MD<sup>2</sup>, Saman Nazarian, MD, PhD<sup>2</sup>, Benoit Desjardins, MD, PhD<sup>4</sup>

<sup>1</sup>Division of Cardiology, Department of Medicine, Taipei Veterans General Hospital, Taipei, Taiwan; Department of Medicine, National Yang-Ming University School of Medicine, Taipei, Taiwan;

<sup>2</sup>Electrophysiology Section, Cardiovascular Division, Department of Medicine, Perelman School of Medicine at the University of Pennsylvania;

<sup>3</sup>Cardiovascular Division, Department of Medicine, University of Pennsylvania School of Medicine;

<sup>4</sup>Department of Radiology, Hospital of Pennsylvania Medical Center, Philadelphia, PA

### Abstract

**Background** —Conflicting data have been reported on the association of left atrial (LA) late gadolinium enhancement (LGE) with atrial voltage in patients with atrial fibrillation. The association of LGE with electrogram (EGM) fractionation and delay remains to be examined. We sought to examine the association between LA LGE on cardiac magnetic resonance (CMR) and EGM abnormalities in patients with atrial fibrillation (AF).

**Methods** —High-resolution LGE CMR was performed prior to EGM mapping and ablation in AF patients. CMR features were quantified using LA myocardial signal intensity z-score (SI-Z), a continuous normalized variable, as well as a dichotomous LGE variable based upon previously validated methodology. EGM mapping was performed pre-ablation during sinus rhythm or LA pacing, and EGM locations were co-registered with CMR images. Analyses were performed using multi-level patient-clustered mixed effects regression models.

**Results** —In the 40 AF patients (age  $63.2 \pm 9.2$  years,  $1312.3 \pm 767.3$  EGM points per patient), lower bipolar voltage was associated with higher SI-Z in patients who had undergone previous ablation (coefficient= $-0.049$ ,  $p < 0.001$ ), but not in ablation-naïve patients (coefficient= $-0.004$ ,  $p = 0.7$ ). LA EGM activation delay was associated with SI-Z in patients with previous ablation (SI-Z: coefficient= $0.004$ ,  $p < 0.001$ ; LGE: coefficient= $0.04$ ,  $p < 0.001$ ) but not in ablation-naïve patients.

**Correspondence:** Benoit Desjardins, MD, PhD, FAHA, FACR, Associate Professor of Radiology and Medicine, Cardiovascular Imaging Section, Department of Radiology, Hospital of Pennsylvania Medical Center, 3400 Spruce Street, Philadelphia, PA 19104, Tel: + 1(215) 615-5476| Fax: + 1(215) 662-7868, benoitd@upenn.edu.

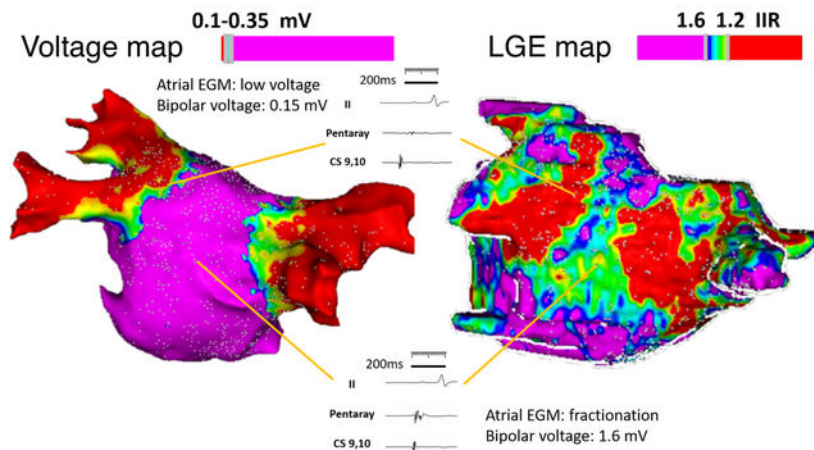
**Disclosures:** Dr. Nazarian is a consultant for CardioSolv and receives software support from Adas and Circle CVI software; he serves as a principal investigator for research funding from Biosense Webster, ImriCor, Siemens, and the US National Heart lung and Blood Institute. The University of Pennsylvania Conflict of Interest Committee manages all commercial arrangements. The other authors report no conflicts of interest.

In contrast, increased LA EGM fractionation was associated with SI-Z (coefficient=0.012,  $p=0.03$ ) and LGE (coefficient=0.035,  $P<0.001$ ) only in ablation-naïve patients.

**Conclusions** —The association of LA LGE with voltage is modified by ablation. Importantly, in ablation naïve patients, atrial LGE is associated with EGM fractionation even in the absence of voltage abnormalities.

### Graphical Abstract

Left atrial LGE on CMR is associated with electrogram abnormalities beyond low voltage in AF patients, which may provide functional reentry targets for ablation.



### Keywords

atrial fibrillation; magnetic resonance imaging; electrophysiology mapping; electrogram fractionation; delayed activation; high-resolution LGE CMR; ADAS-AF

### Journal Subject Terms:

Atrial Fibrillation; Magnetic Resonance Imaging (MRI)

### Introduction

Electrical isolation of pulmonary vein (PV) triggers from the left atrium (LA) is the cornerstone strategy of atrial fibrillation (AF) ablation.<sup>1,2</sup> However, LA myocardial substrates are increasingly recognized to play an important role in AF perpetuation. Previous studies have demonstrated several mechanisms including scar related or functional conduction heterogeneity, and variations in effective refractory periods due to autonomic ganglionated plexus activity.<sup>3, 4</sup> Recent studies support the use of atrial substrate assessment by late gadolinium enhancement (LGE) cardiac magnetic resonance imaging (CMR) for identification of functional reentry substrates and prediction of ablation prognosis.<sup>4-6</sup> Indeed, the extent of LGE on CMR is associated with recurrent AF following ablation.<sup>7</sup> Although an association between complex fractionated atrial electrogram and atrial LGE on CMR has been reported in persistent AF patients,<sup>8</sup> the association of LGE CMR-detected

atrial substrates with intracardiac electrogram (EGM) abnormalities during basal rhythm has rarely been examined.

## Methods

The data that support the findings of this study are available from the corresponding author upon reasonable request.

### Study Population

This study prospectively enrolled drug-refractory symptomatic patients who presented for AF ablation at the Hospital of the University of Pennsylvania between January 2017 and April 2018. The study was approved by an institutional review committee and that all patients gave informed consent for the use of imaging and ablation data for medical research before the procedure.

### CMR Acquisition Protocol

Pre-procedural, 3D navigator-gated LGE CMR was acquired prior to AF ablation. CMR images were performed on a 1.5-Tesla scanner (Avanto, Siemens Medical Imaging, Erlangen, Germany), with a cardiac-phased array receiver surface coil and electrocardiographic gating. Magnetic resonance angiographic TWIST sequence was obtained immediately following injection of 0.2mmol/kg gadoterate meglumine contrast (Dotarem; Guerbet LLC, Bloomington, IN) to define LA and PV anatomy (field-of-view of 340–390mm, echo time of 0.93–0.98ms, repetition time of 2.6ms, in-plane resolution of 1.22×1.22mm, and slice thickness of 1.2mm). LGE CMR images were acquired 15–20 minutes following contrast injection using a 3D inversion-recovery gradient-echo pulse sequence, with respiratory navigation and electrocardiographic gating (field-of-view of 350–390mm, echo time of 1.3–1.6 ms, repetition time of 700–870ms, inversion time of 310–350ms, in-plane resolution of 1.37×1.37mm, and slice thickness of 1.5mm,). The trigger time for the 3D LGE CMR scan was optimized to obtain data during LA diastole with individual adjustment of the inversion time, based upon TI scout, to optimize nulling of LA myocardium.

### CMR Image Analysis

All CMR studies were segmented using ADAS software (Galgo Medical SL, Barcelona, Spain). The LA LGE 3D segmentation process is displayed in Figure 1. The mid LA myocardium was manually contoured on each image. Following identification of the mid LA myocardial contour, the software automatically segmented the LA blood pool by creating an internal contour, which is 5 mm smaller in each radial dimension than the manually drawn mid LA myocardial contour. The signal intensity of voxels on the mid LA myocardial contour were recorded and normalized by dividing the signal intensity of each voxel by the mean blood pool signal intensity to yield the image intensity ratio (IIR), as previously validated.<sup>9</sup> A 3D LA myocardial model was then created using the manual contours. Enhanced myocardial tissues with IIR above 1.2 were defined as atrial LGE. The correlation of atrial substrates detected by electrogram (EGM) mapping and CMR IIR has been

demonstrated previously.<sup>10</sup> Normalized LA signal intensity was also analyzed using signal intensity Z-scores as previously described.<sup>11</sup>

### **Transseptal Access, Mapping and Ablation**

The standard mapping and AF ablation techniques at the Hospital of the University of Pennsylvania have been previously described<sup>12</sup>. Briefly, intravenous heparin was administered to achieve an activated clotting time of >350 s before trans-septal access. Under the guidance of fluoroscopy, two long 8.5 Fr. Trans-septal sheaths (Agilis and SL-1, St. Jude Medical, St. Paul, Minnesota) were advanced over a long guidewire to the superior vena cava and a flushed BRK trans-septal needle (St. Jude Medical) was introduced into the Agilis/SL-1 sheaths. Then, the BRK needle was utilized to puncture through the atrial septum and the whole system was advanced into the LA carefully under fluoroscopy and intra-cardiac echocardiography (ICE, 8 Fr., AcuNav, Biosense Webster, Diamond Bar, California) monitoring. In patients presented in AF, cardioversion was performed before mapping. EAM maps were created during sinus rhythm or distal coronary sinus pacing (LA pacing) using the PentaRay (20 electrodes with 2-6-2 mm spacing) or Lasso catheter (Circular 20-electrodes catheter) by the Carto 3 system (Biosense Webster Inc., Diamond Bar, CA). Mapping was performed with an equal distribution of points using a fill threshold of 15mm. ICE, orthogonal fluoroscopy, and EGM characteristics were used to confirm adequate contact and reliable mapping under sinus rhythm or coronary rhythm per physician's choice. After LA voltage mapping, radiofrequency ablation was performed using a 3.5mm open-irrigated Thermocool®, Thermocool Smarttouch or Thermocool Smarttouch SF (Biosense Webster Inc.) with wide antral PV isolation together with ablation of spontaneous or inducible non-PV triggers<sup>13, 14</sup>. Bidirectional PV entrance and exit block was confirmed and adenosine administration was used to survey acute PV reconnection with further ablation as necessary.

### **Electroanatomic Map Registration**

The segmented LGE-CMR images were co-registered with electroanatomic (EAM) maps using the CartoMerge module (CARTO 3, version 6). Mapping points were extracted from the CARTO workstation and imported into LGE-CMR images utilizing ADAS software. All points were registered and projected onto a LA 3D model off-line to pre-ablation LGE images with sample points. Amongst them, points close to the pulmonary vein, valve, aorta, artifact, overlap of EGMs or no continuous stable EGMs were manually excluded.

Distance between the EGM to the nearest LGE-segmented LA shell was calculated by ADAS software. The continuous SI z-score and LGE dichotomy of the voxels on the mid LA contour neighboring each mapping point were tabulated to evaluate the correlation between voltage, signal intensity, and LGE.

### **Measurements of Atrial Electrogram Characteristics**

Atrial activation time was measured from the reference EGM to the LA point off-line at 200 mm/s speed on the CARTO workstation. The time delay between the proximal coronary sinus atrial signal and the sampled EGM point was measured when mapping during sinus rhythm. On the other hand, activation time was measured from the pacing spike to the

sampled point EGM when mapping during LA pacing at the rate between 650ms to 850ms, slightly faster than the underlying sinus rate. We also sampled forty points that were registered to normal atrial myocardium from the LA anterior and posterior wall in each patient with distance between EAM map and LGE-segmented 3D LA shell model less than 3 mm and compared to all points registered to atrial LGE regions. EGM fractionations were quantified using previously validated methodology<sup>15</sup> for points within 3 mm of the LA shell. EGMs were identified semi-automatically using a custom software. First, all peaks were identified on the bipolar atrial EGMs recorded by catheters, using a peak extraction algorithm.<sup>16</sup> Both positive peaks and negative peaks were separately extracted from the data using parameters that have been manually optimized for the properties of the recorded signal. The results of the peak detection on signal samples were visually verified. Second the set of peaks was parsed to identify individual complexes. Third, the basic parameters for each EGM complex were extracted, such as number of peaks, start and end of EGM. Sample results were again directly visually verified, to make sure they match manual results from experts.

Atrial bipolar EGM deflections exceeding 6 peaks and troughs were defined as abnormally fractionated as illustrated in Figure 2A and the custom software-detected EGM fractionations are displayed in Figure 2B.

### Statistical Analysis

Continuous variables are expressed as mean  $\pm$  standard deviation and categorical variables as number and percentage. The association of EGM characteristics as dependent variables with SI Z-score, and LGE presence were examined using mixed-effects multi-level regression models, clustered by patient. Two-sided p values  $<0.05$  were considered statistically significant. All analyses were performed using STATA version 13 (StataCorp, College Station, Texas).

## Results

### Baseline characteristics, CMR imaging features and procedure data

This study cohort included 40 patients (75% male, mean age  $63.2 \pm 9.2$  years). The baseline clinical, CMR imaging features and procedure data of patients are summarized in Table 1. Thirty-one patients (77.5%) had paroxysmal AF and twenty-four patients (60%) had not undergone a prior ablation. Nine patients (22.5%) presented in AF at the beginning of the procedure and underwent cardioversion before EAM mapping. Twenty-eight patients (80%) acquired EAM voltage mapping during sinus rhythm.

CMR studies were performed at a median of 12 days prior to the procedure (interquartile range: 7.5–21.8 days). The median SI Z-score corresponding to EGM points was  $-0.14$  (IQR:  $-0.6$ – $0.5$ ). The mean of total LA surface area was  $117.8 \pm 30.7$  cm<sup>2</sup> and the mean LA LGE area was  $14.8 \pm 16.3$  cm<sup>2</sup>. Following image to EAM co-registration, the mean registration error was  $2.7 \pm 1.8$  mm.

### Correlation of FAM Voltage and CMR SI

Excluding intra-PV points, 31,334 EGM points were registered to LGE CMR images in total. The mean number of EGM points were  $1312.3 \pm 767.3$  per patient. Of these points, we then focused on 4728 points that were manually identified from the images to satisfy the following criteria: a) adequate distance from the pulmonary veins to exclude venous tissue signal intensity overlap, b) adequate distance from the aorta and mitral valve to exclude image signal intensity bias due to fibrous and vascular tissues, c) lack of any breathing, movement, or slow flow image artifacts, d) a contact signal as determined by two stable electrograms, and e) lack of overlap on adjacent points. The median bipolar voltage was 1.4mV (interquartile range (IQR): 0.8–2.1 mV). In patient clustered, mixed-effects multi-level linear regression models, LA bipolar voltage was negatively associated with SI-Z (coefficient=-0.027,  $z=-4.48$ ,  $p<0.001$ , 95% CI: -0.039 - -0.015. These results were summarized in Table 2. Among all fractionated EGMs, 29.8% were located in low voltage areas (<0.35mV), and 70.2% were located in normal voltage areas.

### Association of CMR Atrial LGE with EGM Abnormalities

The EGM characteristics of points which co-localized to atrial LGE (defined as IIR>1.2) were compared to those registered to the normal myocardium of each patient. Figure 3 displays the EGM characteristics of points projected to the normal myocardium and atrial LGE. Delayed activation and fractionation were observed on EGM points acquired within LA LGE. Interestingly, many EGM points within LGE regions revealed normal bipolar voltage amplitude but increased EGM fractionation as shown in Figure 4. Among ablation naïve patients, higher SI Z-score was associated with increased EGM fractionation while bipolar voltage and delay of EGM activation were not. Furthermore, LGE, defined as IIR>1.2, was also associated with EGM fractionation. Among patients with redo procedures, higher SI-Z was associated with bipolar voltage and delayed atrial EGM activation, but not with EGM fractionation. LGE was also associated with delayed EGM activation (Table 2). Left atrial substrate comparison between EAM voltage map and LGE-CMR are shown in Figure 5.

## Discussion

This study demonstrates that among patients with drug-refractory symptomatic AF with and without prior AF ablation, LA myocardial LGE on CMR is associated with EGM abnormalities beyond low voltage, including delayed activation and fractionation.

### Association of LGE with EGM voltage amplitude

Previous studies have shown an association between LA bipolar endocardial voltage and LGE CMR. Low voltage region size was also associated with the extent of LGE on CMR.<sup>6, 9</sup> Our previous work normalized the measurement of signal intensity on LGE CMR, as IIR, and demonstrated that IIR thresholds of >0.97, >1.20, and >1.61, correspond to voltage <0.5, <0.35, and <0.1 mV, respectively.<sup>9, 17</sup> Zghaib et al.<sup>10</sup> further characterized the correlation between point-by-point (PBP), multipolar mapping and LGE-CMR mapping of left atrium in delineating atrial substrate in AF patients. In the latter study, the 40<sup>th</sup> percentile of voltage amplitude distribution on multipolar mapping was 0.28mV as opposed to 0.42



mV in PBP mapping which suggests that a lower threshold is appropriate with multipolar acquired maps as compared to PBP maps to define the low voltage substrate. Regardless of thresholds, however, some discrepancies between voltage mapping and LGE CMR-detected substrates are often visible and have been reported. Muser et al.<sup>18</sup> illustrated the possibility that abnormal ventricular EGM may be misinterpreted as “normal EGM” according to peak-to-peak bipolar voltage criteria. The presence of high-frequency fractionated near-field components next to lower frequency healthy voltage EGMs is relatively common. Our current clinical practice is to use 0.2–0.45mV as a voltage range indicative of low voltage regions and < 0.2mV as scar on EAM map. However, a simplified view as such is always supplemented by the possibility of “normal” voltage amplitude accompanied with abnormal fractionated components as displayed in Figure 3. Integration of LGE CMR into the clinical workflow may enhance our ability to find such substrates not readily identified by voltage mapping. Indeed, our study suggests that among patients with prior ablation, atrial LGE mainly exhibit scar from ablation. Our prior work has shown that scar from ablation often exhibits higher intensity and decreased wall thickness when compared to regions with pre-existing fibrosis.<sup>19</sup> Ostial regions with LGE gaps correlated to PV reconnection (not necessarily the earliest signal) on EAM. However, as previously reported by our group,<sup>20</sup> the presence of LGE did not preclude the presence of reconnection. This is explained by the limited resolution of CMR, which may not detect small conducting fibers in the ablation path. The current study also demonstrates that EGM fractionation is associated with *de novo* LA LGE, but unassociated with ablation scar LGE.

A prior study by Jadidi *et al.*<sup>21</sup> suggested that EGM fractionation in sinus and coronary sinus-paced rhythms often results from wave collision, which means many fractionated EGMs are functional in nature and unassociated with fixed structural abnormalities. Accordingly, they concluded that targeting all fractionated LA EGMs during sinus rhythm or coronary sinus-pacing is an inappropriate strategy. Our results showed a strong association between LA LGE and EGM fractionation, which suggests that at least some sites with EGM fractionation exhibit poor contrast reuptake despite normal voltage and LA LGE likely signify structural changes such as expanded extracellular space, fat infiltration, or inflammation. Strikingly, the EGM fractionations specifically correlate with *de novo* LGE and not previous ablation scar. These atrial substrates may enhance functional reentry and AF perpetuation. Beyond the current mainstream ablation strategy – PV isolation, and various patient-tailored AF substrate ablation approaches—focal impulse and rotor modulation,<sup>22–24</sup> complex fractionated EGM modification<sup>25</sup>, dominant-frequency ablation,<sup>26</sup> and low bipolar voltage area modification,<sup>27, 28</sup> LGE on CMR may also indicate arrhythmogenic sites as potential ablation targets.

At present, there are various methods and software to define atrial LGE by LGE-CMR. In addition to the IIR method as described above,<sup>9</sup> the full width at half maximum (FWHM) technique and n-standard deviation thresholds above the mean signal in the nulled myocardium, are also performed to detect LGE CMR atrial substrates and applied to patient-tailored ablation strategies.<sup>6, 29,30</sup> One of the great challenges in streamlining research and clinical applications in this area is the development of a standardized methodology with adequate generalizability, reproducibility, and accuracy. Future collaboration among investigators is necessary to achieve this task.

We believe our results lend further mechanistic support to the ongoing prospective, multicenter study: DECAAF II (), which is designed to compare the conventional PVI ablation to PVI plus fibrosis-guided ablation in 888 persistent AF patients and we await the results of this exciting study.

### Study Limitations

The current study has several limitations. First, this is a single-center study with a relatively small sample size. Due to the small sample size, the statistical models did not adjust for potential confounders. However, given the analytic method that clustered data at the patient level to examine within patient association of EGM characteristics with signal intensity z-scores and a validated binary variable based on LGE, no known significant potential confounders are anticipated. Second, our results may be influenced by the accuracy of CMR-segmented LA image to EAM map registration. However, the registration process was optimized by “landmark” registration with three distinct anatomic points, followed by “surface” registration. The accuracy of image registration by this approach had been previously validated.<sup>31</sup> Third, the gold standard to define atrial scar is confirmed by tissue histology as muscle bundles which are replaced and interspaced by connective tissue.<sup>32</sup> Such histology is unavailable in observational studies of patients undergoing AF ablation. However, we do not claim any association between LGE and specific histologic changes. Rather, we report an association between EGM abnormalities previously recognized to underlie functional and fixed reentry, and LGE. Fourth, atrial activation does not occur sequentially between coronary sinus to the sampled atrial EGM during sinus rhythm which may bias the measurement of activation delay. However, EGM timing in the coronary sinus relative to timing in the high right atrium was stable throughout the ablation procedure. Also, the onset of p wave was obscure in severely diseased atrium. To standardize the calculation of time delay of atrial EGM, we chose the coronary sinus EGM as our reference. Fifth, of all patients 70% underwent voltage mapping during sinus rhythm and 30% underwent voltage mapping during distal coronary sinus pacing. Importantly, the rhythm and thus direction of propagation stayed stable within each patient and statistical comparisons are clustered per patient, taking into account any variability that may be due to interpatient differences in propagation direction.

### Conclusions

The association of LA LGE with voltage is modified by ablation. Atrial LGE is associated with delayed EGM activation and fractionation even in the absence of voltage abnormalities. Identification of atrial LGE by CMR illustrates physiological significance and may provide functional reentry targets for ablation.

### Supplementary Material

Refer to Web version on PubMed Central for supplementary material.

### Sources of Funding:

Dr. Kuo is supported by Taipei Veterans General Hospital-National Yang-Ming University Excellent Physician Scientists Cultivation Program, No. 106-V-A-009. The study was also funded by a Biosense Webster Grant to Dr



Nazarian and the Koegel Family EP Research Fund. Dr. Nazarian's research laboratory is also supported by NIH grants R01HL116280 and R01HL142893, which indirectly supported this research. The contents do not necessarily represent the views of the National Institutes of Health.

## Non-standard Abbreviations and Acronyms

<b>AF</b>	atrial fibrillation
<b>CMR</b>	cardiac magnetic resonance
<b>EGM</b>	electrogram
<b>IIR</b>	image intensity ratio
<b>LA</b>	left atrium
<b>LGE</b>	late gadolinium enhancement
<b>PV</b>	pulmonary vein
<b>PBP</b>	point-by-point
<b>SI-Z</b>	signal intensity z-score

## Reference:

1. Calkins H, Hindricks G, Cappato R, Kim YH, Saad EB, Aguinaga L, Akar JG, Badhwar V, Brugada J, Camm J, et al. 2017 hrs/ehra/ecas/aphrs/solaece expert consensus statement on catheter and surgical ablation of atrial fibrillation: Executive summary. *J Arrhythm.* 2017;33:369–409. [PubMed: 29021841]
2. Calkins H, Kuck KH, Cappato R, Brugada J, Camm AJ, Chen SA, Crijns HJ, Damiano RJ Jr., Davies DW, DiMarco J, et al. 2012 hrs/ehra/ecas expert consensus statement on catheter and surgical ablation of atrial fibrillation: Recommendations for patient selection, procedural techniques, patient management and follow-up, definitions, endpoints, and research trial design. *Europace.* 2012;14:528–606. [PubMed: 22389422]
3. Miyamoto K, Tsuchiya T, Narita S, Yamaguchi T, Nagamoto Y, Ando S, Hayashida K, Tanioka Y, Takahashi N. Bipolar electrogram amplitudes in the left atrium are related to local conduction velocity in patients with atrial fibrillation. *Europace.* 2009;11:1597–1605. [PubMed: 19910315]
4. Cochet H, Dubois R, Yamashita S, Al Jefairi N, Berte B, Sellal JM, Hooks D, Frontera A, Amraoui S, Zemoura A, et al. Relationship between fibrosis detected on late gadolinium-enhanced cardiac magnetic resonance and re-entrant activity assessed with electrocardiographic imaging in human persistent atrial fibrillation. *JACC Clin Electrophysiol.* 2018;4:17–29. [PubMed: 29479568]
5. Khurram IM, Habibi M, Gucuk Ipek E, Chrispin J, Yang E, Fukumoto K, Dewire J, Spragg DD, Marine JE, Berger RD, et al. Left atrial lge and arrhythmia recurrence following pulmonary vein isolation for paroxysmal and persistent af. *JACC Cardiovasc Imaging.* 2016;9:142–148. [PubMed: 26777218]
6. Oakes RS, Badger TJ, Kholmovski EG, Akoum N, Burgon NS, Fish EN, Blauer JJ, Rao SN, DiBella EV, Segerson NM, et al. Detection and quantification of left atrial structural remodeling with delayed-enhancement magnetic resonance imaging in patients with atrial fibrillation. *Circulation.* 2009;119:1758–1767. [PubMed: 19307477]
7. Marrouche NF, Wilber D, Hindricks G, Jais P, Akoum N, Marchlinski F, Kholmovski E, Burgon N, Hu N, Mont L, et al. Association of atrial tissue fibrosis identified by delayed enhancement mri and atrial fibrillation catheter ablation: The decaaf study. *JAMA.* 2014;311:498–506. [PubMed: 24496537]
8. Hwang SH, Oh YW, Lee DI, Shim J, Park SW, Kim YH. Relation between left atrial wall composition by late gadolinium enhancement and complex fractionated atrial electrograms in

patients with persistent atrial fibrillation: Influence of non-fibrotic substrate in the left atrium. *Int J Cardiovasc Imaging*. 2015;31:1191–1199. [PubMed: 25957631]

9. Khurram IM, Beinart R, Zipunnikov V, Dewire J, Yarmohammadi H, Sasaki T, Spragg DD, Marine JE, Berger RD, Halperin HR, et al. Magnetic resonance image intensity ratio, a normalized measure to enable interpatient comparability of left atrial fibrosis. *Heart Rhythm*. 2014;11:85–92. [PubMed: 24096166]
10. Zghaib T, Keramati A, Chrispin J, Huang D, Balouch MA, Ciuffo L, Berger RD, Marine JE, Ashikaga H, Calkins H, et al. Multimodal examination of atrial fibrillation substrate: Correlation of left atrial bipolar voltage using multi-electrode fast automated mapping, point-by-point mapping, and magnetic resonance image intensity ratio. *JACC Clin Electrophysiol*. 2018;4:59–68. [PubMed: 29520376]
11. Xie S, Desjardins B, Kubala M, Liang J, Yang J, van der Geest RJ, Schaller R, Riley M, Callans D, Zado E, et al. Association of regional epicardial right ventricular electrogram voltage amplitude and late gadolinium enhancement distribution on cardiac magnetic resonance in patients with arrhythmogenic right ventricular cardiomyopathy: Implications for ventricular tachycardia ablation. *Heart Rhythm*. 2018;15:987–993. [PubMed: 29501666]
12. Dixit S, Lin D, Frankel DS, Marchlinski FE. Catheter ablation for persistent atrial fibrillation: Antral pulmonary vein isolation and elimination of nonpulmonary vein triggers are sufficient. *Circ Arrhythm Electrophysiol*. 2012;5:1216–1223; discussion 1223. [PubMed: 23250551]
13. Santangeli P, Zado ES, Hutchinson MD, Riley MP, Lin D, Frankel DS, Supple GE, Garcia FC, Dixit S, Callans DJ, et al. Prevalence and distribution of focal triggers in persistent and long-standing persistent atrial fibrillation. *Heart Rhythm*. 2016;13:374–382. [PubMed: 26477712]
14. Santangeli P, Marchlinski FE. Techniques for the provocation, localization, and ablation of non-pulmonary vein triggers for atrial fibrillation. *Heart rhythm : the official journal of the Heart Rhythm Society*. 2017;14:1087–1096.
15. Zghaib T, Ipek EG, Zahid S, Balouch MA, Misra S, Ashikaga H, Berger RD, Marine JE, Spragg DD, Zimmerman SL, et al. Association of left atrial epicardial adipose tissue with electrogram bipolar voltage and fractionation: Electrophysiologic substrates for atrial fibrillation. *Heart Rhythm*. 2016;13:2333–2339. [PubMed: 27546816]
16. Duarte Marcos, from the Laboratory of Biomechanics and Motor Control at the Federal University of ABC in Brazil. <http://nbviewer.ipython.org/github/demotu/BMC/blob/master/notebooks/DetectPeaks.ipynb>.
17. Dewire J, Khurram IM, Pashakhanloo F, Spragg D, Marine JE, Berger RD, Ashikaga H, Rickard J, Zimmerman SL, Zipunnikov V, et al. The association of pre-existing left atrial fibrosis with clinical variables in patients referred for catheter ablation of atrial fibrillation. *Clin Med Insights Cardiol*. 2014;8:25–30. [PubMed: 25368540]
18. Muser D, Santangeli P, Liang JJ, Castro SA, Magnani S, Hayashi T, Garcia FC, Frankel DS, Dixit S, Zado ES, et al. Characterization of the electroanatomic substrate in cardiac sarcoidosis: Correlation with imaging findings of scar and inflammation. *JACC Clin Electrophysiol*. 2018;4:291–303. [PubMed: 30089553]
19. Fukumoto K, Habibi M, Gucuk Ipek E, Khurram IM, Zimmerman SL, Zipunnikov V, Spragg DD, Ashikaga H, Rickard J, Marine JE, Berger RD, et al. Comparison of preexisting and ablation-induced late gadolinium enhancement on left atrial magnetic resonance imaging. *Heart Rhythm*. 2015;12:668–672. [PubMed: 25533586]
20. Spragg DD, Khurram I, Zimmerman SL, Yarmohammadi H, Barcelon B, Needleman M, Edwards D, Marine JE, Calkins H, Nazarian S. Initial experience with magnetic resonance imaging of atrial scar and co-registration with electroanatomic voltage mapping during atrial fibrillation: Success and limitations. *Heart Rhythm*. 2012;9:2003–2009. [PubMed: 23000671]
21. Jadidi AS, Duncan E, Miyazaki S, Lellouche N, Shah AJ, Forclaz A, Nault I, Wright M, Rivard L, Liu X, et al. Functional nature of electrogram fractionation demonstrated by left atrial high-density mapping. *Circ Arrhythm Electrophysiol*. 2012;5:32–42. [PubMed: 22215849]
22. Narayan SM, Krummen DE, Shivkumar K, Clopton P, Rappel WJ, Miller JM. Treatment of atrial fibrillation by the ablation of localized sources: Confirm (conventional ablation for atrial fibrillation with or without focal impulse and rotor modulation) trial. *J Am Coll Cardiol*. 2012;60:628–636 [PubMed: 22818076]

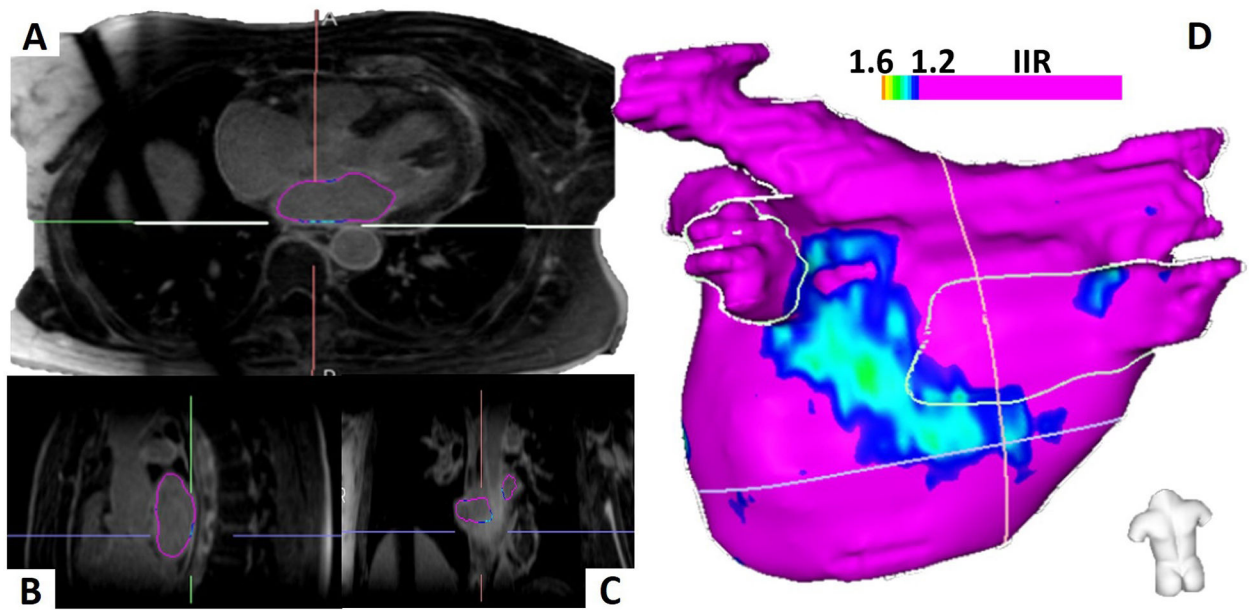
23. Buch E, Share M, Tung R, Benharash P, Sharma P, Koneru J, Mandapati R, Ellenbogen KA, Shivkumar K. Long-term clinical outcomes of focal impulse and rotor modulation for treatment of atrial fibrillation: A multicenter experience. *Heart Rhythm*. 2016;13:636–641. [PubMed: 26498260]
24. Lin YJ, Lo MT, Chang SL, Lo LW, Hu YF, Chao TF, Chung FP, Liao JN, Lin CY, Kuo HY, et al. Benefits of atrial substrate modification guided by electrogram similarity and phase mapping techniques to eliminate rotors and focal sources versus conventional defragmentation in persistent atrial fibrillation. *JACC Clin Electrophysiol*. 2016;2:667–678. [PubMed: 29759744]
25. Verma A, Mantovan R, Macle L, De Martino G, Chen J, Morillo CA, Novak P, Calzolari V, Guerra PG, Nair G, et al. Substrate and trigger ablation for reduction of atrial fibrillation (star af): A randomized, multicentre, international trial. *Eur Heart J*. 2010;31:1344–1356. [PubMed: 20215126]
26. Jarman JW, Wong T, Kojodjojo P, Spohr H, Davies JE, Roughton M, Francis DP, Kanagaratnam P, Markides V, Davies DW, et al. Spatiotemporal behavior of high dominant frequency during paroxysmal and persistent atrial fibrillation in the human left atrium. *Circ Arrhythm Electrophysiol*. 2012;5:650–658. [PubMed: 22722660]
27. Rolf S, Kircher S, Arya A, Eitel C, Sommer P, Richter S, Gaspar T, Bollmann A, Altmann D, Piedra C, et al. Tailored atrial substrate modification based on low-voltage areas in catheter ablation of atrial fibrillation. *Circ Arrhythm Electrophysiol*. 2014;7:825–833. [PubMed: 25151631]
28. Blandino A, Bianchi F, Grossi S, Biondi-Zoccai G, Conte MR, Gaido L, Gaita F, Scaglione M, Rametta F. Left atrial substrate modification targeting low-voltage areas for catheter ablation of atrial fibrillation: A systematic review and meta-analysis. *Pacing Clin Electrophysiol*. 2017;40:199–212. [PubMed: 28054377]
29. Hwang SH, Oh YW, Lee DI, Shim J, Park SW, Kim YH. Evaluation of quantification methods for left atrial late gadolinium enhancement based on different references in patients with atrial fibrillation. *Int J Cardiovasc Imaging*. 2015;31 Suppl 1:91–101. [PubMed: 25367893]
30. Harrison JL, Jensen HK, Peel SA, Chiribiri A, Grondal AK, Bloch LO, Pedersen SF, Bentzon JF, Kolbitsch C, Karim R, et al. Cardiac magnetic resonance and electroanatomical mapping of acute and chronic atrial ablation injury: A histological validation study. *Eur Heart J*. 2014;35:1486–1495. [PubMed: 24419806]
31. Bertaglia E, Brandolino G, Zoppo F, Zerbo F, Pascotto P. Integration of three-dimensional left atrial magnetic resonance images into a real-time electroanatomic mapping system: Validation of a registration method. *Pacing Clin Electrophysiol*. 2008;31:273–282. [PubMed: 18307621]
32. Boldt A, Wetzel U, Lauschke J, Weigl J, Gummert J, Hindricks G, Kottkamp H, Dhein S. Fibrosis in left atrial tissue of patients with atrial fibrillation with and without underlying mitral valve disease. *Heart*. 2004;90:400–405. [PubMed: 15020515]

**What is Known**

- The association of left atrial late gadolinium enhancement with voltage is modified by ablation.
- Left atrial late gadolinium enhancement on cardiac magnetic resonance imaging is associated with electrogram fractionation and/or delay.

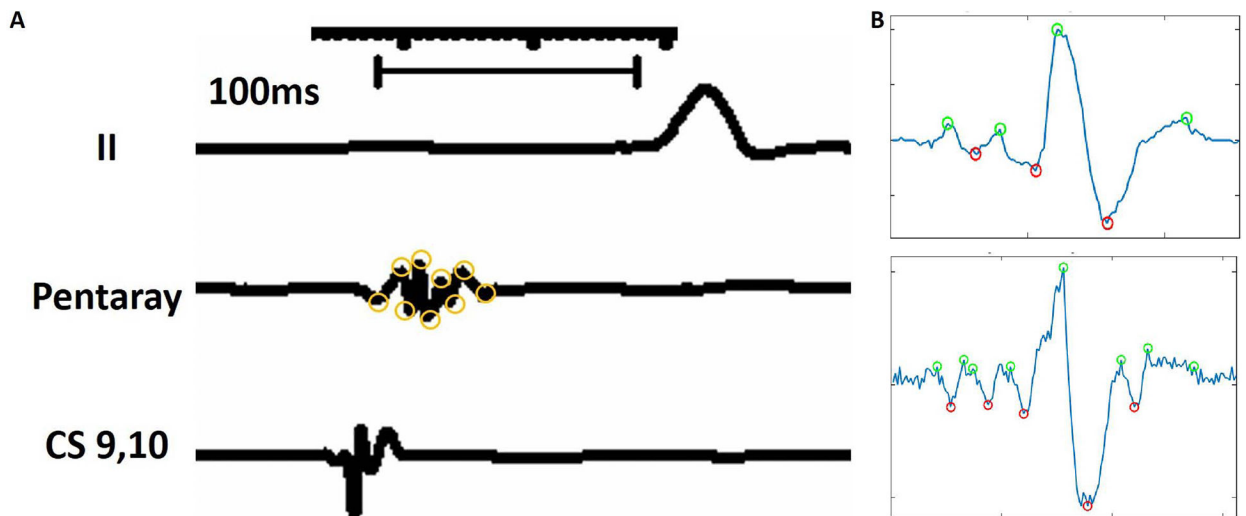
**“What the Study Adds”**

- Identification of left atrial late gadolinium enhancement on cardiac magnetic resonance imaging can associate with the abnormal electrogram beyond voltage in atrial fibrillation patients, which may serve as functional reentry and lends mechanistic support to current studies to target abnormal substrates.



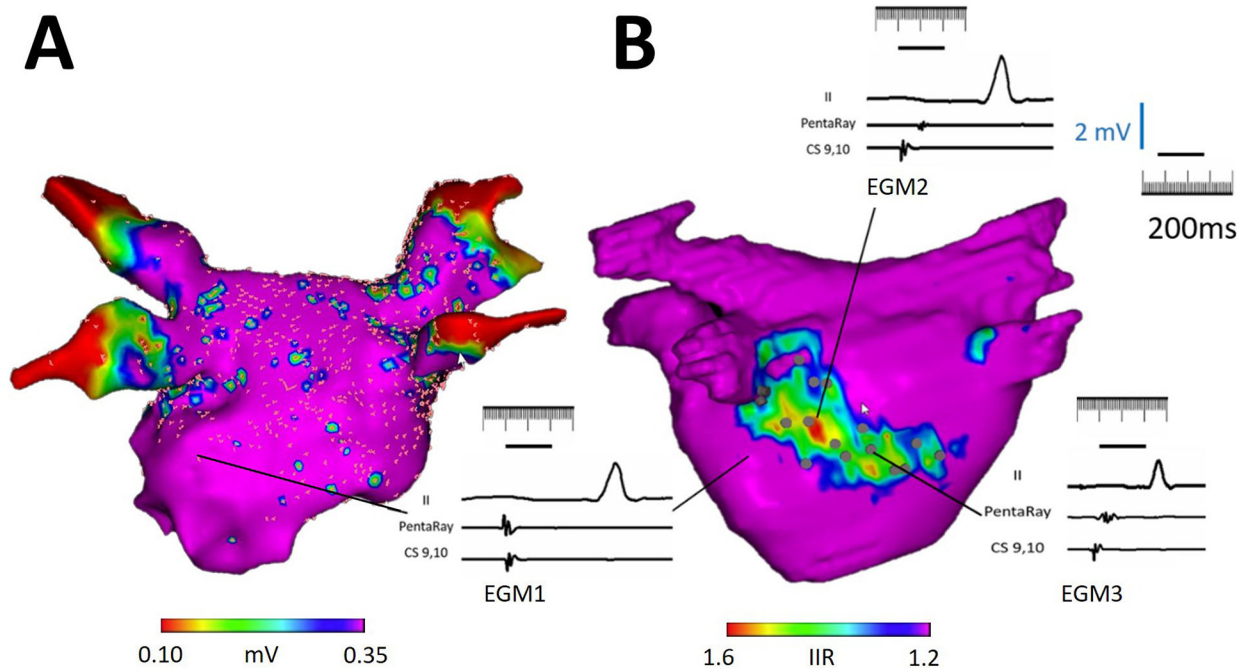
**Figure 1.**

Left Atrial Segmentation and Three-Dimensional Left Atrium Model. The left atrium is manually contoured on three-dimensional, high-resolution late gadolinium enhancement cardiac magnetic resonance images and visualized in all three axes (A-C). The left atrial three-dimensional model with posterior wall substrate in an ablation-naive patient is displayed (D).



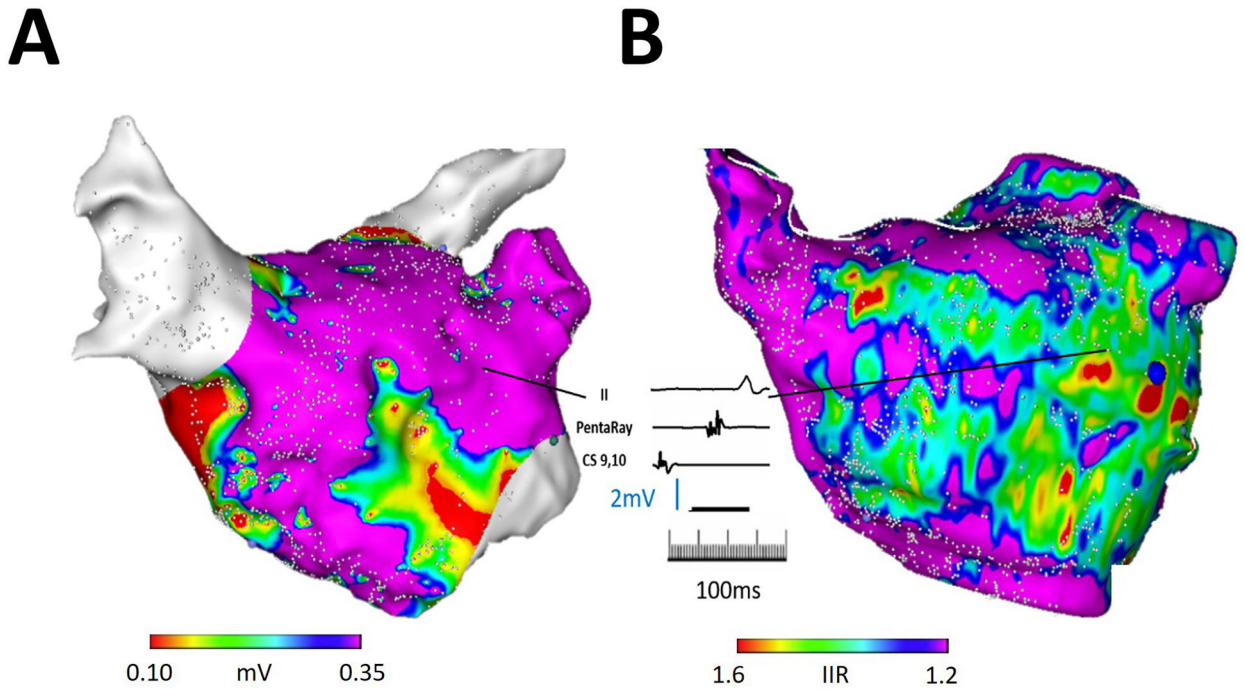
**Figure 2.** Definition of fractionated atrial electrograms. The figure illustrates the measurement process for the number of deflections within each electrogram. Electrograms were displayed at a sweep speed of 200 ms. Then the number of deflections was measured as the number of peaks plus troughs. In this example, 9 deflections are noted on the atrial electrogram recording, consistent with abnormal electrogram fractionation.





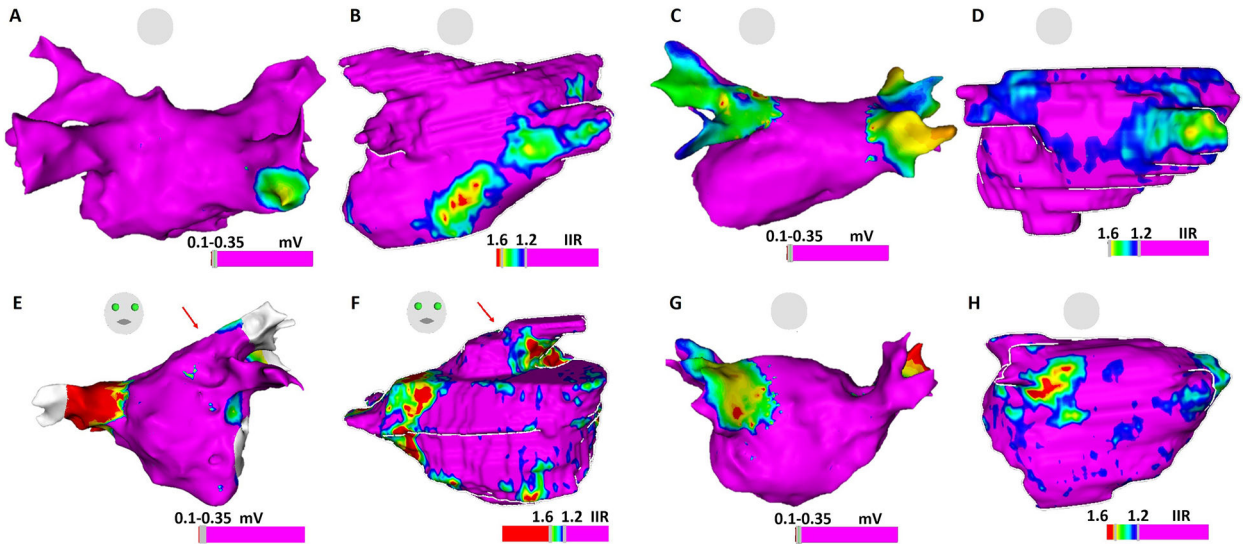
**Figure 3.**

Illustration of CMR LGE-detected atrial substrate and EGM characteristics. (A) The panel shows a postero-anterior view of a left atrial bipolar voltage map, which is registered to the left atrial CMR segmentation from panel B. Note that the voltage map shows no significant cohesive low amplitude areas within the left atrial body. (B) The panel demonstrates the left atrial CMR segmentation with color thresholds defined by image intensity ratio (IIR) from the same patient. The bipolar voltage map from panel A is hidden. Electrograms acquired from points corresponding to predefined IIR thresholds are displayed. A normal EGM is noted in a region with IIR < 1.2 as EGM 1. A delayed and fractionated EGM with borderline low voltage is noted in a region with IIR > 1.6 as EGM 2. Importantly, a large region with intermediate IIR (between 1.2 to 1.6) displayed normal bipolar voltage (>0.50mV) with fractionated EGMs suggestive of electrical disease (EGM 3).



**Figure 4.**

Illustration of CMR LGE-detected atrial substrate and EGM characteristics. (A) The panel demonstrates an anteroposterior view of an electroanatomic left atrial map in a patient with prior pulmonary vein isolation. Regions with low voltage are noted surrounding but not encircling the pulmonary veins, as well as in the septal peri-mitral area. (B) The panel demonstrates left atrial CMR segmentation from the same patient with color thresholds defined by IIR in the same orientation as in panel A. A representative electrogram acquired from a point corresponding to IIR between 1.2–1.6 and normal bipolar voltage (1.38mV) demonstrates fractionation and >80 ms delay compared to the proximal coronary sinus signal suggestive of electrical disease.



**Figure 5.**

Comparison of atrial substrate on EAM voltage map and LGE-CMR shell. Panels 5A and 5B: ablation-naïve patient with normal LA voltage but increased EGM fractionation on posterior LGE region on CMR shell; Panels 5C and 5D: Re-do ablation patient with chronic isolated right PVs and reconnected left PVs, compatible with low voltage at the antrum of right PVs on EAM and abnormal atrial myocardium on LGE-CMR; Panels 5E and 5F: Re-do ablation patient with normal voltage, but delayed atrial EGMs (arrow) on left PV antrum, corresponding to the atrial substrate (arrow) on LGE-CMR; Panels 5G and 5H: Electrical reconnection of right PVs. EGMs shows normal voltage at right PV antrum. Few EGMs show delayed activation at scarce atrial substrate region on CMR.

**Table 1.**

Baseline Characteristics, CMR imaging features and Procedure data

<b>Baseline Characteristics</b>	
N	40
Age (years)	63.2 ± 9.2
Male (%)	30 (75)
Paroxysmal atrial fibrillation (%)	31 (77.5)
Left ventricular ejection fraction (%)	59.2 ± 6.1
Hypertension (%)	23 (57.5)
Diabetes mellitus (%)	2 (5)
Congestive heart failure (%)	2 (5)
Ischemic stroke/transient ischemic attack (%)	5 (12.5)
Coronary artery disease (%)	5 (12.5)
Chronic obstructive pulmonary disease (%)	3 (7.5)
Obstructive sleep apnea (%)	8 (20)
Peripheral artery disease (%)	3 (7.5)
CHA2DS2-VASc score	2.0 ± 1.2
0	2 (5)
1	15 (37.5)
2	11 (27.5)
3	7 (17.5)
4	3 (7.5)
5	2 (5.0)
Prior ablation	0.6 ± 0.9
0	24 (60)
1	9 (22.5)
2	5 (12.5)
3	2 (5)
<b>Cardiac Magnetic Resonance imaging features</b>	
Left atrium volume measured by CMR (ml)	80.3 ± 29.7
Late Gadolinium Enhancement area (IIR>1.2), cm <sup>2</sup>	14.8 ± 16.3
Late Gadolinium Enhancement area (IIR>1.2), %	12.6 ± 13.2
Late Gadolinium Enhancement area (IIR>1.6), cm <sup>2</sup>	1.4 ± 3.1
Late Gadolinium Enhancement area (IIR>1.6), (%)	1.1 ± 2.6
Signal intensity z-score of sampled points (IQR)	-0.14 (-0.6-0.5)
<b>Procedure data</b>	
Mapping rhythm: Sinus rhythm (%)	28 (70)
Electroanatomical map points	1312.3 ± 767.3
Electroanatomical map points for analysis	123.9 ± 120.4

Baseline Characteristics	
Bipolar Voltage mV (IQR: 25–75 quartile)	1.4 (0.8–2.1)

IQR: interquartile range

Author Manuscript

Author Manuscript

Author Manuscript

Author Manuscript

**Table 2.** Association of Electrogram Abnormalities with Signal Intensity Z Scores and IIR defined Atrial Substrate

	Beta Coefficient	Standard Error	Z	P> z	Lower 95% CI	Upper 95% CI
<b>Total population, n=40</b>						
Bipolar voltage (mV)	-0.027	0.006	-4.48	<0.001	-0.039	-0.015
Delayed atrial electrogram activation	0.003	0.001	5.41	<0.001	0.002	0.004
Atrial electrogram fractionation	0.006	0.004	1.65	0.1	-0.001	0.013
<b>Ablation-naïve group, n=24</b>						
Bipolar voltage (mV)	-0.004	0.009	-0.44	0.7	-0.021	0.014
Delayed atrial electrogram activation	0.002	0.001	1.63	0.1	<-0.001	0.004
Atrial electrogram fractionation	0.012	0.006	2.13	<b>0.03</b>	0.001	0.024
<b>Redo ablation group, n=16</b>						
Bipolar voltage (mV)	-0.049	0.009	-5.42	<0.001	-0.067	-0.032
Delayed atrial electrogram activation	0.004	0.001	4.85	<0.001	0.002	0.005
Atrial electrogram fractionation	0.001	0.005	0.2	0.8	-0.009	0.01
<b>Left atrium LGE (IIR &gt;1.2)</b>						
<b>Total population, n=40</b>						
Delayed atrial electrogram activation	0.024	0.002	14.39	<0.001	0.021	0.027
Atrial electrogram fractionation	0.008	0.006	1.36	0.2	-0.004	0.02
<b>Ablation-naïve group, n=24</b>						
Delayed atrial electrogram activation	<-0.001	0.001	-0.53	0.6	-0.001	0.001
Atrial electrogram fractionation	0.035	0.008	4.55	<0.001	0.02	0.051
<b>Redo ablation group, n=16</b>						
Delayed atrial electrogram activation	0.04	0.004	10.92	<0.001	0.033	0.047
Atrial electrogram fractionation	-0.005	0.011	-0.48	0.6	-0.026	0.016

IQR: interquartile range; CI: confidence interval